Hindawi
Mathematical Problems in Engineering
Volume 2022, Article ID 9451091, 11 pages
https://doi.org/10.1155/2022/9451091

Research Article

Intelligent Computing of Levenberg-Marquard Technique Backpropagation Neural Networks for Numerical Treatment of Squeezing Nanofluid Flow between Two Circular Plates

Hakeem Ullah,[1] **Mehreen Fiza**,[1] **Muhammad Asif Zahoor Raja**,[2] **Imran Khan**,[1] **Muhammad Shoaib**,[3] **and Seham M. Al-Mekhlafi**[4]

[1]*Department of Mathematics, Abdul Wali Khan University, Mardan 23200, KP, Pakistan*
[2]*Future Technology Research Center, National Yunlin University of Science and Technology, 123 University Road, Section 3, Douliou, Yunlin 64002, Taiwan*
[3]*Department of Mathematics, COMSATS University Islamabad, Attock Campus, Attock 43600, Pakistan*
[4]*Department of Mathematics, Sana'a University, Sana'a, Yemen*

Correspondence should be addressed to Mehreen Fiza; drmehreenfiza@gmail.com and Seham M. Al-Mekhlafi; smdk100@gmail.com

Received 7 March 2022; Revised 25 June 2022; Accepted 6 July 2022; Published 19 August 2022

Academic Editor: Arshad Riaz

This study presents new techniques based on the artificial intelligence neural network with Levenberg-Marquardt Scheme with backpropagation (ANN-LMS). The boundary value problem BVP is obtained from the governing equations of the flow model. Along with ANN-LMS, the semianalytical method namely the optimal homotopy analysis method (OHAM) is used for validating the results. ANN-LMS optimized the absolute error and increased the accuracy of the solution. The effect of physical parameters is discussed with the help of plots and tables.

1. Introduction

The squeezing flow has many important applications in engineering, material science, and physics. The squeezing flow has captured the imagination of many scientists and engineers in recent years due to its frequent applications in industrial and engineering such as stirring pistons, squeezed film and polymer manufacturing, sweet fillers, hydraulic lift, electric motors, flow within the nozzle and nasogastric tube, power transmission, modeling of chewing and eating, heart values and blood vessels [1–6]. Stefan [7] initiated pioneering works in this direction. Verma [8] examined the numerical solution of squeezing flow between the two plates. Sheikholeslami et al. [9] used the Adomian decomposition method (ADM) to explore the unsteady squeezing flow of nanofluids. Gupta and Ray [10] investigated the unsteady squeezing flow of nanofluid between two parallel plates numerically. The squeezing flow of a second-grade fluid was investigated by Rajagopal and Gupta [11]. Hayat et al. [12] investigated the squeezing flow of second-grade material by two disks. Hayat et al. [13] presented a three-dimensional squeezing flow between two parallel plates with mixed convection. The squeezing flow of electrically conducting fluids between parallel plates under the influence of a magnetic field has been studied extensively in recent years. Siddiqui et al. [14] adopted the homotopy perturbation method and investigated the magnetic effect of squeezing viscous magnetohydrodynamics (MHD) fluid flow. Ahmed et al. [15] investigated MHD squeezing flow of Casson fluid between parallel disks. For the solutions of the system of ODEs/PDEs, both the analytical and numerical methods are in practice. The numerical methods required linearization and discretization techniques which distress the accuracy. The AI-based numerical technique was frequently used in different applications to solve differential equations [16–18], but there is a need to explore and exploit the stochastic

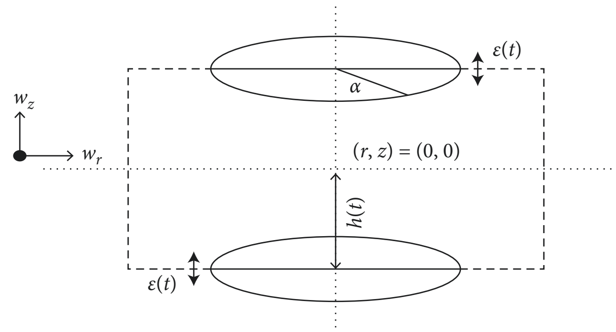

FIGURE 1: Flow diagram.

numerical technique based on intelligent computing paradigms to solve and analyze the problems given in Equations (14)–(16). A few recently published studies of paramount importance contain mathematical model solution in nonlinear optics [19], atomic physics [20], and financial models [21, 22], eye model [23], COVID-19 virus spread models [24, 25], entropy generation system [26, 27], and flow problems [28–40]. According to our literature research, to examine the SFNM between two circular plates, we apply the AI technique through the ANN-LMS to realize nonlinear backpropagation of neural network to Equations (14)–(16). This outlines the creative features of the emerging computing model as follows:

(1) A unique two-layer feed-forward backpropagation of ANN-LMS is proposed for the analysis of squeezed flow between two circular plates
(2) The MSE-based merit function is planned for the realization of ANN-LMS for estimated modeling of squeezed flow between two circular plates by means of the PF, TT, FT, and VL reference dataset
(3) The accurate, consistent, and convergent PR of the constructed proposal ANN-LMS is authenticated for the problem while the solver values are further authorized by the error analysis and EH and RG studies.

2. Flow Analysis

Let us assume an incompressible squeezing flow between two circular disks with separation $2s(t)$. The plane for the mentioned flow is suggested as $(\tilde{z}, \tilde{r})$ plane, and the plate movements are about the central axis $\tilde{z} = 0$, and the axisymmetric is about $\tilde{r} = 0$. The plate movement is about the z axis which is symmetric and nonrotating as shown in Figure 1.

The velocity field is given as $V = (u(r, z, t), 0, w(r, z, t))$. The governing equations are given as follows:

$$
\begin{gathered}
\frac{1}{r}\partial_r (ru) + \partial_z w = 0, \\
(\partial_t u + u\partial_r u + w\partial_z u) = -\frac{\partial_r p}{\rho} + \nu\left(\nabla^2 u - \frac{u}{r^2}\right), \\
(\partial_t w + u\partial_r w + w\partial_z w) = -\frac{\partial_z p}{\rho} + \nu\left(\nabla^2 w\right).
\end{gathered} \tag{1}
$$

With BCs,

$$
\begin{aligned}
&u = 0, w = v_c \quad z = h, \\
&\partial_z u = 0, w = 0 \quad z = 0,
\end{aligned} \tag{2}
$$

where v_c is the velocity of circular plates and $\overline{\nabla}^2$ as dell operator also using the nondimensional variable $\eta = z/h$ and $u = -rv_c/2h(t)f'(\eta)$, $\quad w = v_c f(\eta)$. The governing equations becomes

$$
\begin{gathered}
f^{'''}{}' + R(\eta - f)f^{'''} + 2f'' - Qf'' = 0, \\
R = \frac{h\varepsilon}{v}, Q = \frac{h^2}{vc}\frac{d\varepsilon}{dt}, \\
f(1) = 1, f'(1) = 0, \\
f(0) = 0, f''(0) = 0.
\end{gathered} \tag{3}
$$

3. Numerical Results and Explanation

This section provides a concise explanation of the approach used, and the results of the numerical simulations received through the backpropagated supervised network ANN-LMS designed for the fluid flow system represented via 14–15 based on SFNM. The six steps of the proposed methodology's step-by-step process flow are shown in Figure 2. The 201 input grid between the closed intervals of 0 and 1 is used to produce the proposal dataset for ANN-LMS for the problem. Presently, 10% of the data are used for TT, 10% for VL, and 80% of the data are used at random for TR. Neural network-based supervised learning is constructed after constructing the data through Equations (14)–(15). TR data are utilized to formulate the estimated solution based on an MSE-based merit function. This article presents numerical experimentation for the ANN-LMM for SFNM between two plates that are circular. For one scenario, in the g, the design of the ANN-LMM is used as shown in Tables 1 and 2. The "nts" method of Matlab's neural network toolbox is used to create ANN-LMS, which has a two-layer feed-forward network structure with backpropagation. Figure 3 depicts the structural layout for the designed network, which uses the concept of the hidden layer through activation function and appropriated adjustments of weights.

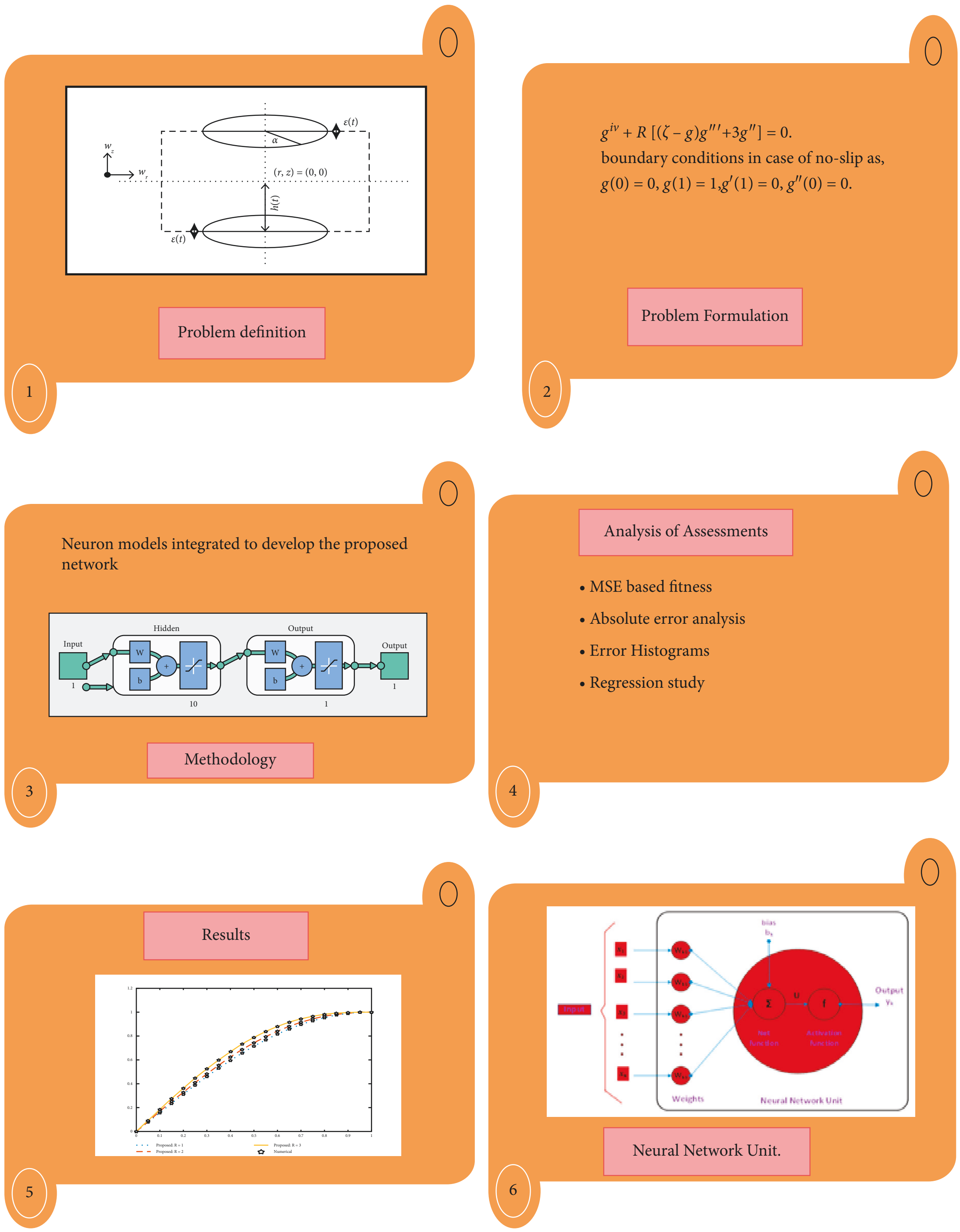

Figure 2: (1–6): Operational flow between two circular plates for the proposed ANN-LMS for SFNM.

In Figures 4–7, for the scenario one case one of f and f' results of ANN-LMS, error histogram, and FT are shown, respectively. In Figure 8, the RG analysis of SFNM between two plates that are circular is shown. For case one scenario one, there is a convergence of MSE for TR, VL, and TT progression in Figures 4(a) and 4(b). This scenario involves one SFNM between two circular plates. In Tables 3 and 4, for the scenario one case, one different numerical values are

Table 1: Values of physical quantities affecting f for the fluid flow problem under consideration.

Physical quantities R	Scenarios	Cases
1		1
3	1	2
5		3

Table 2: Values of physical quantities effecting f' for the fluid flow problem under consideration.

Physical quantities R	Scenarios	Cases
1		1
3	1	2
5		3

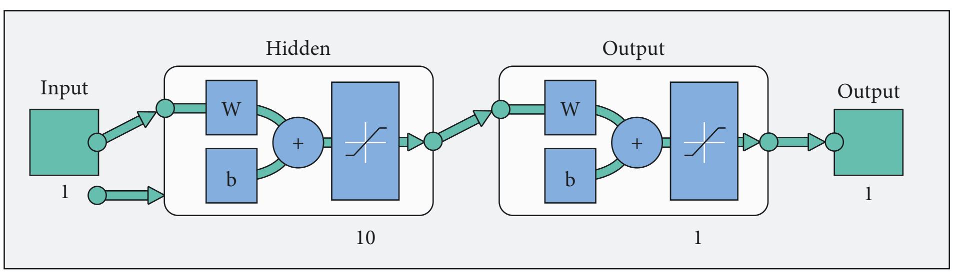

Figure 3: Networks flow diagram.

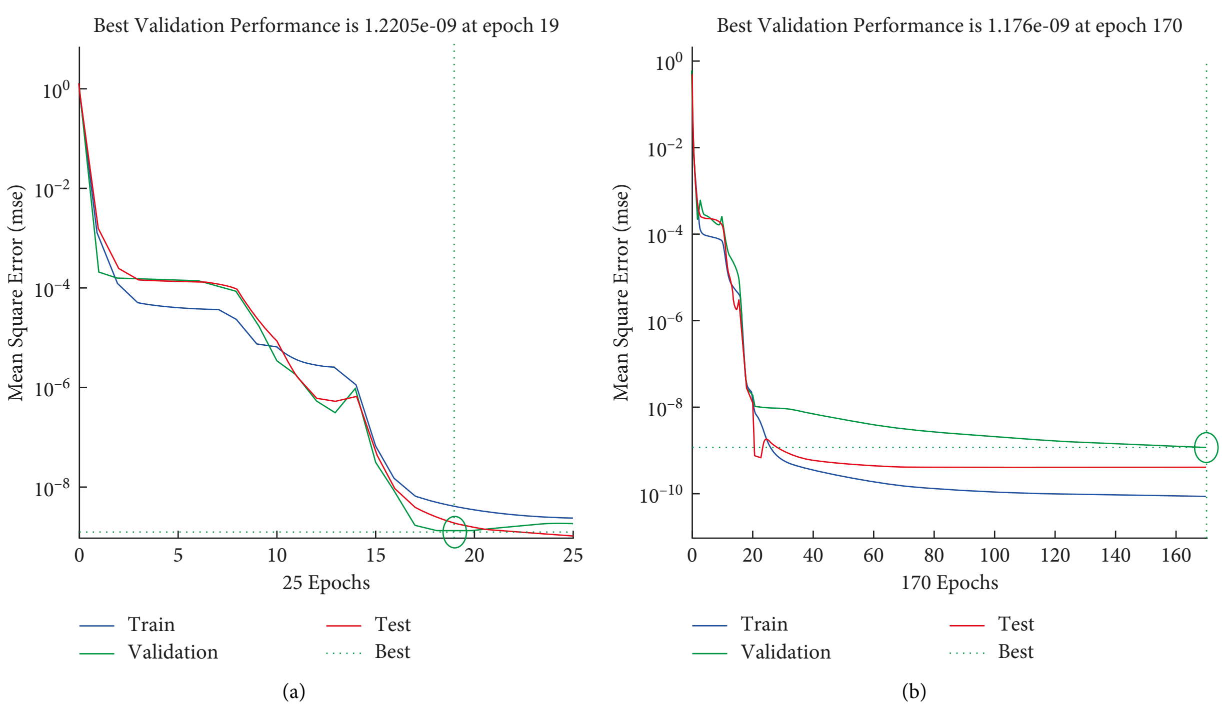

Figure 4: Case one of scenario one SFNM between two circular plates, PF result of MSE for proposed ANN-LMS.

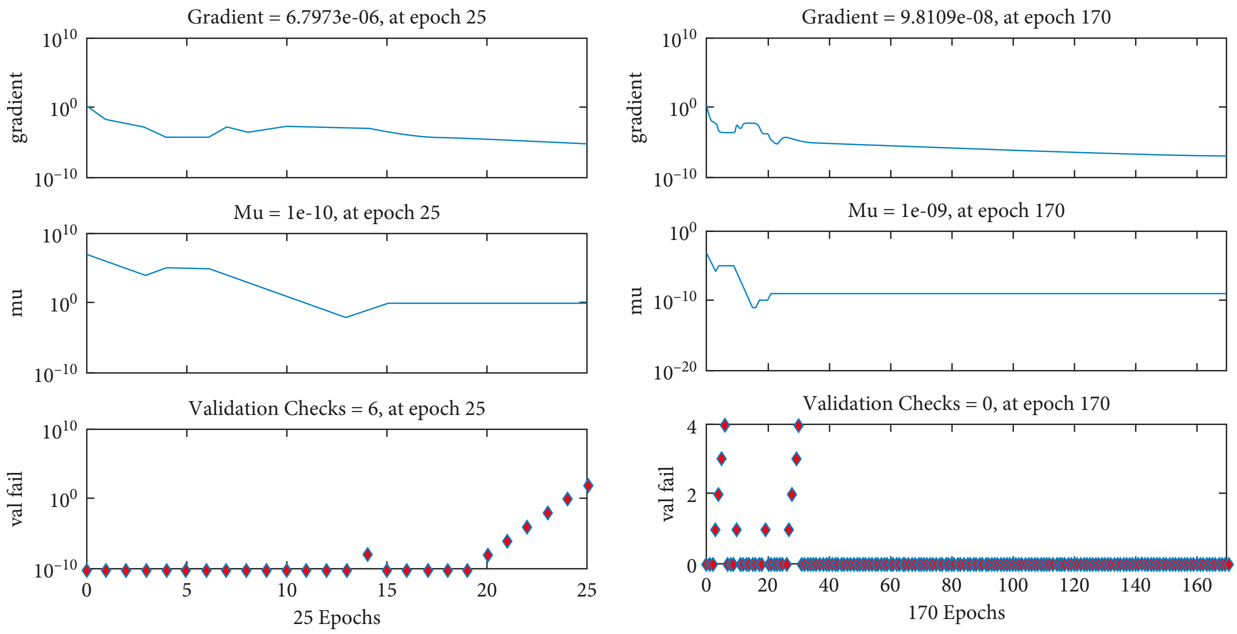

(a) (b)

Figure 5: The outcome of the intended ANN-state LMS's transition dynamic for the first scenario (case1).

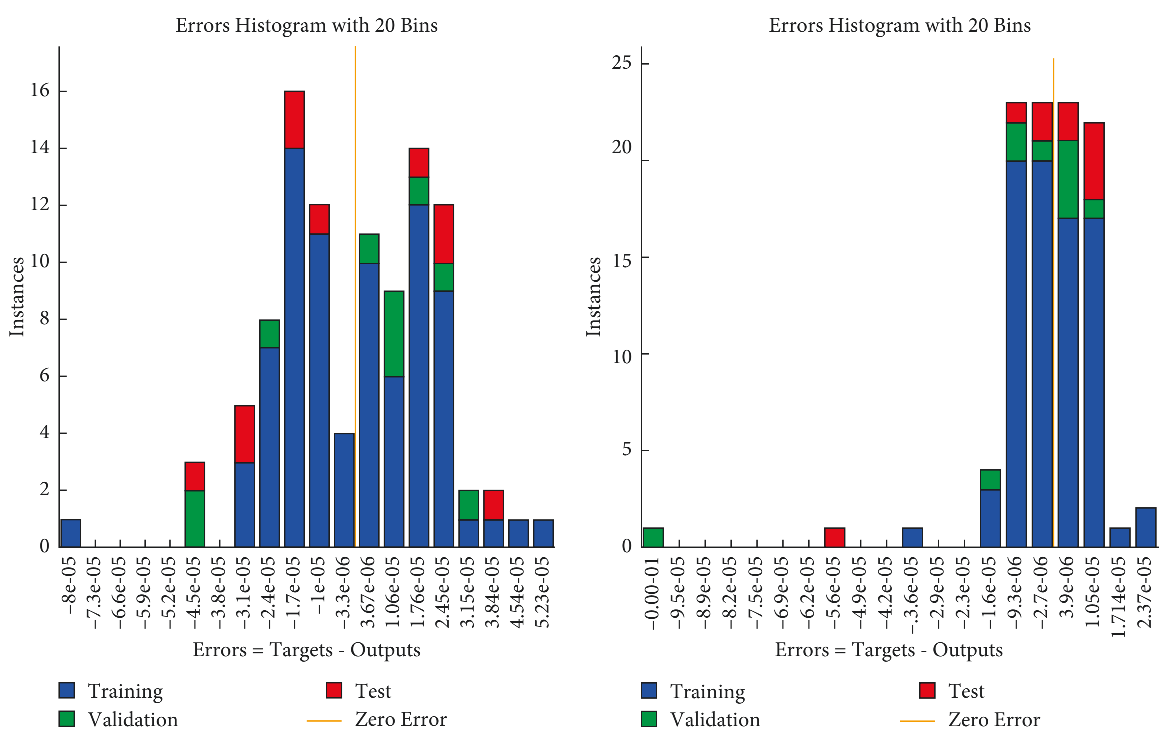

(a) (b)

Figure 6: EH representation against first scenario (case1).

presented. We noticed that at epochs 170, the greatest network PF are $1.176e^{-9}$, and at epoch 19 $1.2e^{-9}$, respectively. In Figures 5(a) and 5(b), the back-gradient propagation's and step size Mu are approximately (at the epochs 25 and at the epochs 170) and (10^{-10}, 10^{-9}), respectively. The ANN-LMS′ PF-generated results are

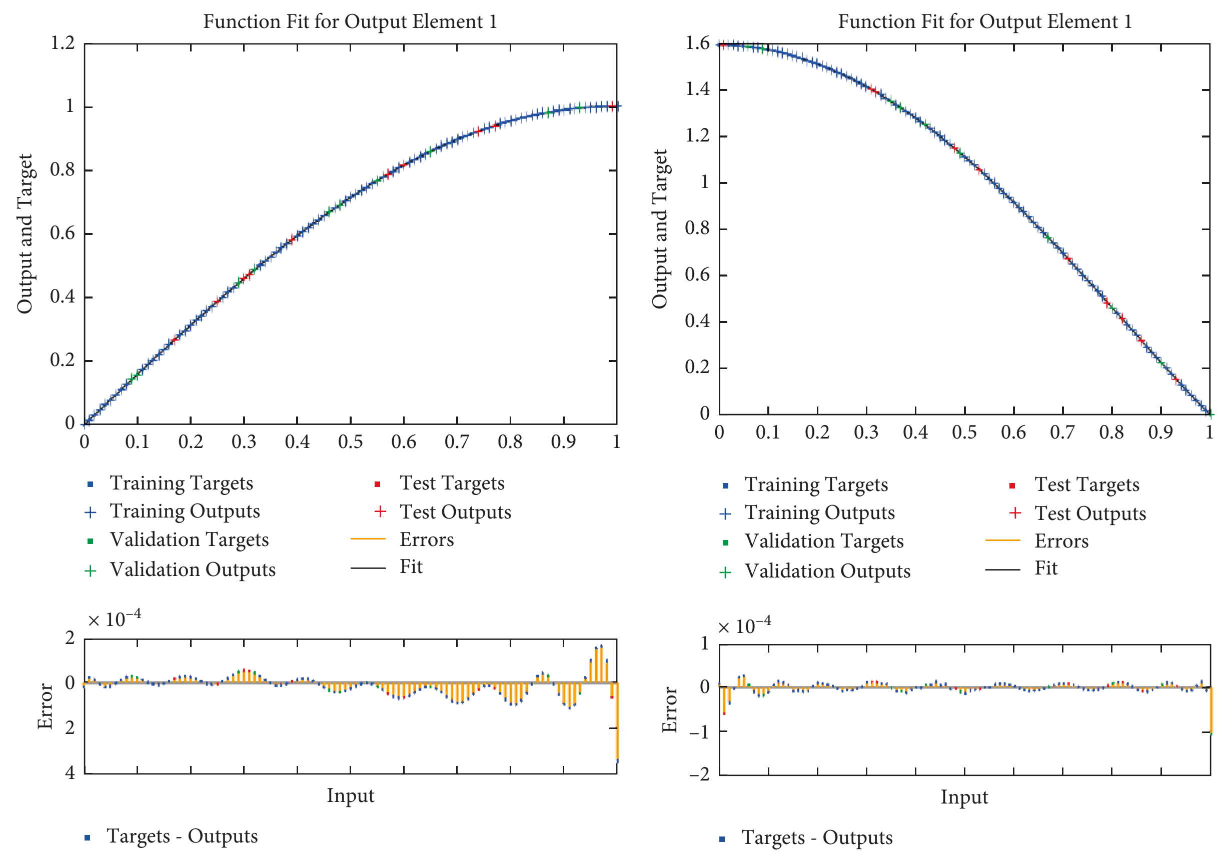

(a) (b)

Figure 7: FTs representation against first scenario (case1).

Table 3: Results for scenario 1 of the flow problem for *f*.

Case	MSE Training	Validation	Testing	Performance	Gradient (E)	Mu (E)	Epoch	Time
1	3.85913$E-10$	8.05434$E-10$	4.08718$E-10$	8.61$E-11$	9.81−8	1−9	270	0
2	1.744$E-9$	6.13895$E-9$	3.05430$E-8$	1.74$E-9$	9.99−8	1−8	245	0
3	4.408$E-10$	6.56798$E-10$	7.06632$E-10$	4.41$E-10$	9.98−8	1−9	241	0

Table 4: Results for scenario 1 of the flow problem *f*'.

Case	MSE Training	Validation	Testing	Performance	Gradient (E)	Mu	Epoch	Time
1	8.60809$E-11$	1.17599$E-9$	4.08718$E-10$	8.61$E-11$	9.88−8	1$E-9$	278	0
2	8.3733$E-9$	5.74998$E-9$	1.34309$E-8$	5.81$E-12$	1.00−8	1$E-11$	220	0
3	7.891$E-11$	5.34501$E-11$	9.06819$E-11$	4.789$E-11$	1.43−8	1$E-9$	1000	3

examined along with a numerical recommendation from the OHAM technique against Scenario 1 (first case). Figures 7(a) and 7(b) show the outcomes in terms of solution and errors. Step size is 0.01 for the domain values lies between 0 and 1. Figure 8 reflects the outcomes of Regression for the scenario 1 of the flow problem. Figures 6(a) and 6(b) corresponding to scenario 1 (first case) represent the error analysis through EH. The maximum error that the intended ANN-LMS can accomplish for TT, TR, and VL data is less than 1 e^4 and 4 e^4 for case one scenario one of the system model. R values for correlations are always close to one. Tables 3 and 4 show the results of the fluid flow system ANN-LMS approach for

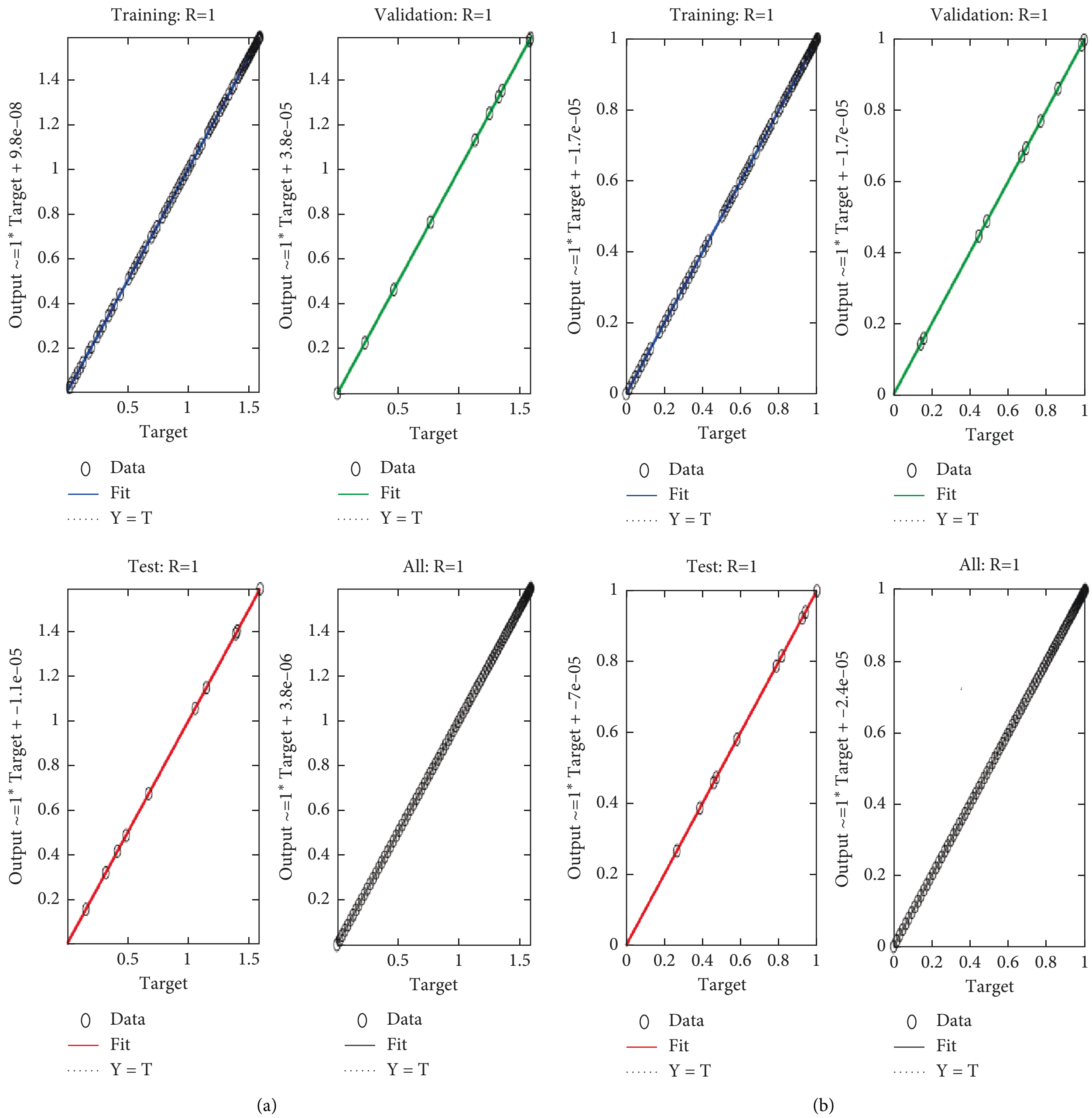

Figure 8: FTs representation against first scenario (case1).

resolving Case 1 and scenario one of the SFNM. For scenarios one and case one of SFNM between two circular plates, the PF of ANN-LMS is approximately 10^{-11}, 10^{-12}, and 10^{-9} to 10^{-10}. These results show that ANN-LMS can solve SFNM between two circular plates with a reliable PF. In light of this, scenario one's velocity profiles and ANN-LMS results are calculated. Figures 9–10 are constructed for the outcomes $f(\zeta)$ and $f(\zeta)$. As a consequence of the ANN-coordination LMMs with standard OHAM solutions in Case 1 and Scenario 1, the absolute error from orientation solutions has been determined, and the results are displayed in Figures 9(b) and 10(b) for scenario one case one. Absolute errors for the $f(\zeta)$ and $f(\zeta)$ are 10^{-4} to 10^{-7}, 10^{-3} to 10^{-05}, 10^{-5} to 10^{-6}, and 10^{-3} to 10^{-6}, 10^{-4} to 10^{-6}, 10^{-4} to 10^{-5}, respectively. The absoulte errors ofscenario 1 for f and f' are 10-3 to 10-6, 10-4 to 10-6, 10-4 to 10-5, and 10-4 to 10-7, 10 -3 to 10-05 , 10-5 to 10-6, respectively. As the plates come together, the pressure between them is greater than the pressure in the center, and vice versa. The pressure differential for various values of R is shown in Figure.

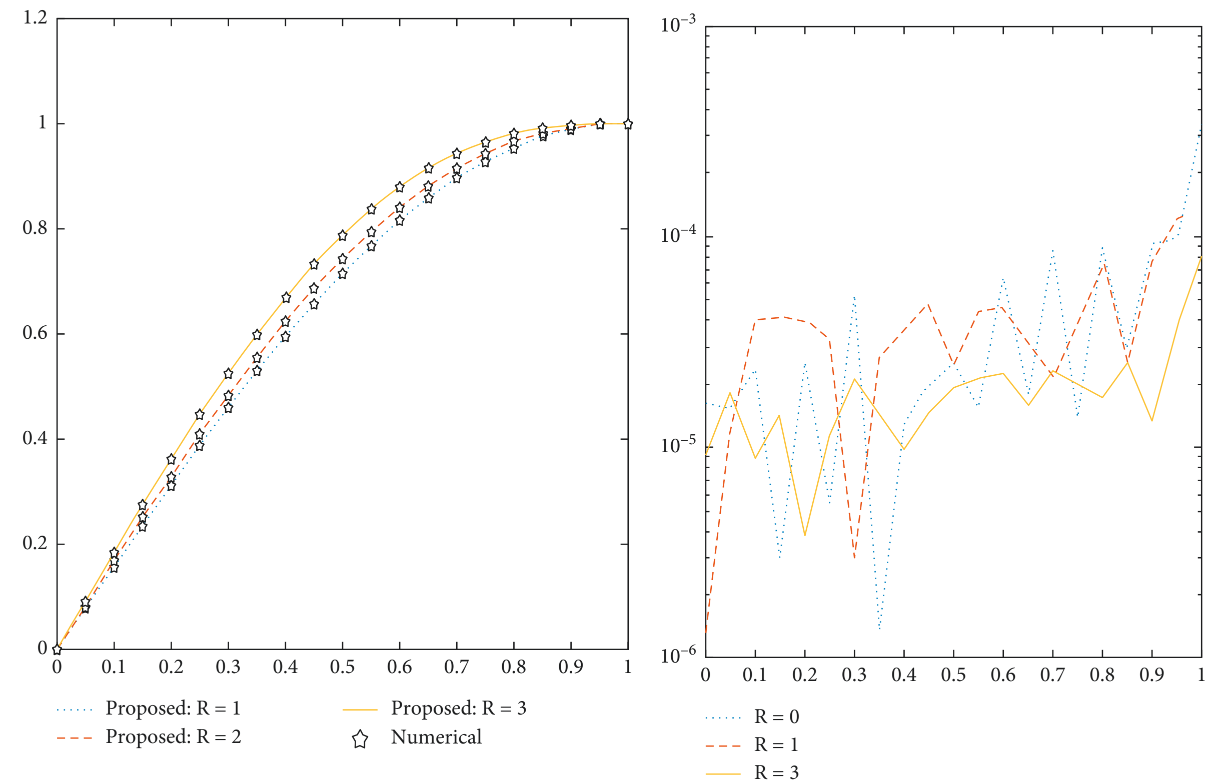

(a) (b)

FIGURE 9: A comparison of OHAM and ANN-LMS is presented along with a suggested numerical result corresponding to the first scenario for g.

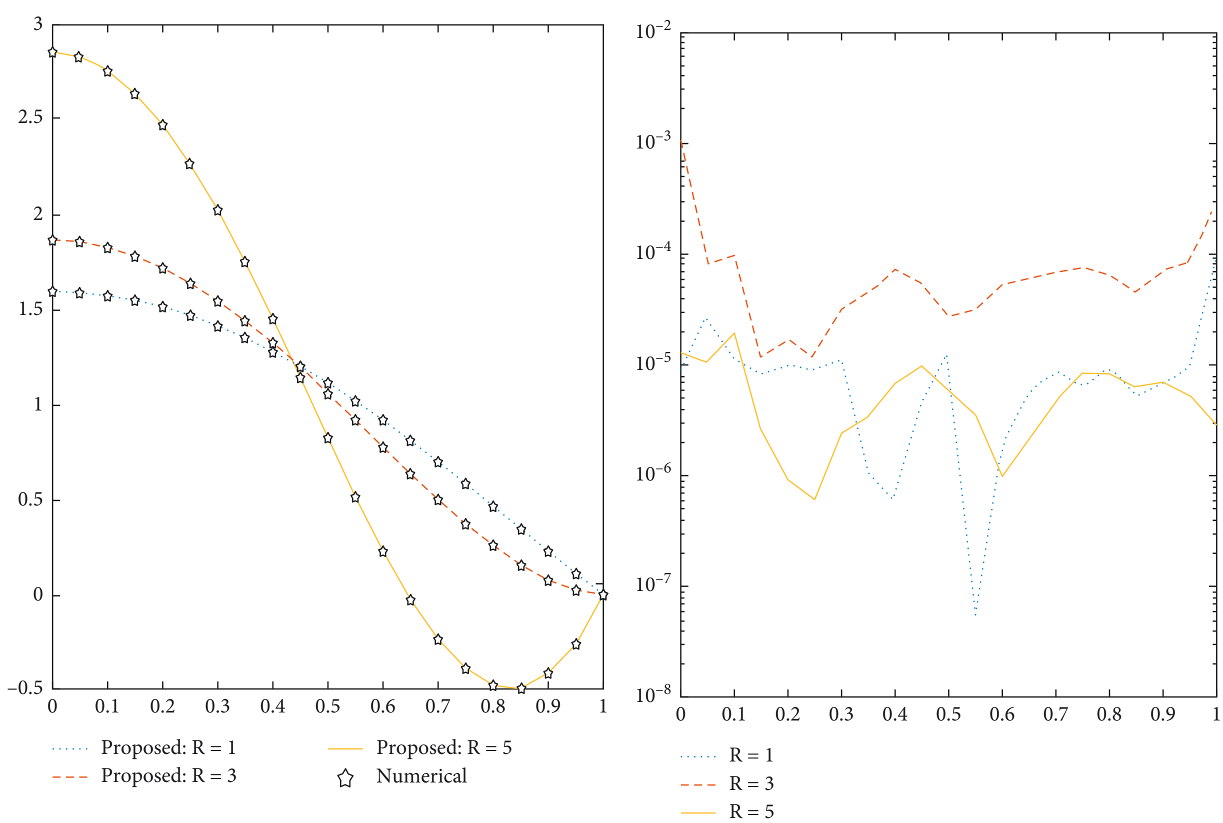

(a) (b)

FIGURE 10: OHAM and ANN-LMS solutions comparison with suggested numerical results for scenario 1.

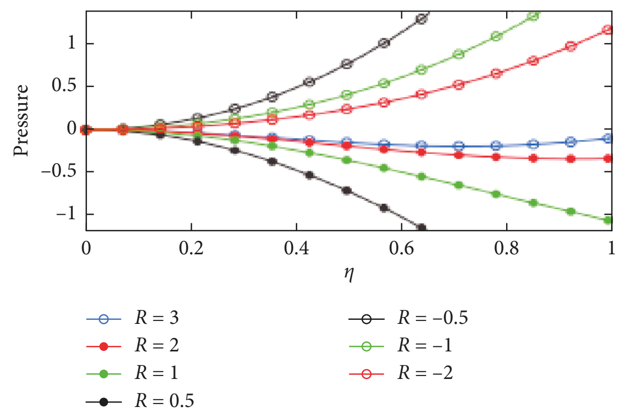

FIGURE 11: Variation of pressure for different values of R.

4. Concluding Remarks

Intelligence-based intellectual computing backpropagation provides an alternative environment for the solution of fluid flow problem under consideration in terms of performance plots, regression metrics, gradient analysis, and error dynamics through histograms consisting of a variety of bins. The followings are the main results of the study:

(1) As the plates become closer to one another, the pressure between them rises more than the pressure in the centre and vice versa

(2) Velocity profile depicts the opposite trends corresponding to positive and negative values of Reynolds number

(3) The selction of dataset such as 80% fortraining, 10% for validation and 10% for testing proves that our method is stable, relaiable, and fast convergent than the other methods

(4) Pressure rises in the direction towards the middle region between two plates when both plates get closer to each other.

(5) By contrasting the results with a numerical method, the method's validity is established (Runge–Kutta method having order 4)

(6) The initial guess and linearization methods are not necessary for ANN-LMS

(7) Due to its ability to reduce accuracy and absolute error, ANN-LMS performs better than other approaches

Future direction: the authors are motivated to work on new unsupervised learning algorithms after successful completion of work representing supervised learning [34–36].

Nomenclature

ANNs: Artificial neural network
SF: Squeezing flow
υ: Kinematic viscosity
NN: Neural network
BL: Boundary layer
k: Thermal conductive
BVP: Boundary value problem
Pr: Prandtl number
Eh: Epoch MSE mean square error
ρ: Fluid density
μ: Dynamic viscosity
PF: Performance
TT: Testing
TR: Training
VD: Validation
EB: Error bin
EH: Histogram
GD: Gradient
RG: Regression
AE: Absolute error
Ep: Epoch
MSE: Mean square error.

Data Availability

All the relevant data are presented in the paper.

Conflicts of Interest

The authors declare that they have no conflicts of interest.

References

[1] P. S. Gupta and A. S. Gupta, "Squeezing flow between parallel plates," *Wear*, vol. 45, no. 2, pp. 177–185, 1977.

[2] R. T¨ornqvist, P. Sunderland, and J. A. E. Manson, "Nonisothermal process rheology of thermoplastic composites for compression flow moulding," *Composites Part A: Applied Science and Manufacturing*, vol. 31, no. 9, pp. 917–927, 2000.

[3] P. Shirodkar, A. Bravo, and S Middleman, "Lubrication flows in viscoelastic liquids: 2. Effect of slip on squeezing flow between approaching parallel rigid planes," *Chemical Engineering Communications*, vol. 14, no. 3–6, pp. 151–175, 1982.

[4] Y. Tian, S Wen, and Y Meng, "Compressions of electrorheological fluids under different initial gap distances," *Physical Review A*, vol. 67, no. 5, Article ID 051501, 2003.

[5] R. B. Bird, R. C. Armstrong, and O. Hassager, "Dynamics of polymeric liquids," *Fluid Mechanics*, vol. 1, 1987.
[6] J. L. Kokini, J. B. Kadane, and E. L. Cussler, "Liquid texture perceived in the mouth," *Journal of Texture Studies*, vol. 8, no. 2, pp. 195–218, 1977.
[7] M. J. Stefan, "Versuchs Uber die scheinbare adhesion, Sitzungsberichte der Akademie der Wissenschaften in Wien," *Mathematik-Naturwissen*, vol. 69, pp. 713–721, 1874.
[8] R. L. Verma, "A numerical solution for squeezing flow between parallel channels," *Wear*, vol. 72, no. 1, pp. 89–95, 1981.
[9] M. Sheikholeslami, D. D. Ganji, and H. R. Ashorynejad, "Investigation of squeezing unsteady nanofluid flow using ADM," *Powder Technology*, vol. 239, pp. 259–265, 2013.
[10] A. K. Gupta and S. S. Ray, "Numerical treatment for investigation of squeezing unsteady nanofluid flow between two parallel plates," *Powder Technology*, vol. 279, pp. 282–289, 2015.
[11] K. R. Rajagopal and A. S. Gupta, "Remarks on "a class of exact solutions to the equations of motion of a second grade fluid"," *International Journal of Engineering Science*, vol. 21, no. 1, pp. 61–63, 1983.
[12] T. Hayat, A. Yousaf, M. Mustafa, and S. Obaidat, "MHD squeezing flow of second-grade fluid between two parallel disks," *International Journal for Numerical Methods in Fluids*, vol. 69, no. 2, pp. 399–410, 2012.
[13] T. Hayat, A. Qayyum, and A. Alsaedi, "Three-dimensional mixed convection squeezing flow," *Applied Mathematics and Mechanics*, vol. 36, no. 1, pp. 47–60, 2015.
[14] A. M. Siddiqui, S. Irum, and A. R. Ansari, "Unsteady squeezing flow of viscous MHD fluid between parallel plates," *Mathematical Modelling and Analysis*, vol. 13, no. 4, pp. 565–576, 2008.
[15] N. Ahmed, U. Khan, X. J. Yang, S. I. U. Khan, Z. A. Zaidi, and S. T. Mohyud-Din, "Magneto hydrodynamic (MHD) squeezing flow of a Casson fluid between parallel disks," *International Journal of the Physical Sciences*, vol. 8, no. 36, pp. 1788–1799, 2013.
[16] M. A. Z. Raja, I. Ahmad, I. Khan, M. I. Syam, and A. M. Wazwaz, "Neuro-heuristic computational intelligence for solving nonlinear pantograph systems," *Frontiers of Information Technology & Electronic Engineering*, vol. 18, no. 4, pp. 464–484, 2017.
[17] Z. Sabir, M. A. Z. Raja, M. Umar, and M. Shoaib, "Neuro-swarm intelligent computing to solve the second-order singular functional differential model," *The European Physical Journal Plus*, vol. 135, no. 6, p. 474, 2020.
[18] Y. Wang, Y. Cao, Z. Guo, and S. Wen, "Passivity and passification of memristive recurrent neural networks with multi-proportional delays and impulse," *Applied Mathematics and Computation*, vol. 369, Article ID 124838, 2020.
[19] I. Ahmad, S. Ahmad, M. Awais, S. Ul Islam Ahmad, and M. Asif Zahoor Raja, "Neuro-evolutionary computing paradigm for Painlevé equation-II in nonlinear optics," *The European Physical Journal Plus*, vol. 133, no. 5, p. 184, 2018.
[20] S. u. I. Ahmad, F. Faisal, M. Shoaib, and M. A. Z. Raja, "A new heuristic computational solver for nonlinear singular Thomas–Fermi system using evolutionary optimized cubic splines," *European Physical Journal A: Hadrons and Nuclei*, vol. 135, no. 1, p. 55, 2020, https://doi.org/10.1140/epjp/s13360-019-00066-3.
[21] A. H. Bukhari, M. A. Z. Raja, M. Sulaiman, S. Islam, M. Shoaib, and P. Kumam, "Fractional neuro-sequential ARFIMA-LSTM for financial market forecasting," *IEEE Access*, vol. 8, pp. 71326–71338, 2020.
[22] A. Ara, N. A. Khan, O. A. Razzaq, T. Hameed, and M. A. Z. Raja, "Wavelets optimization method for evaluation of fractional partial differential equations: an application to financial modelling," *Advances in Difference Equations*, vol. 2018, no. 1, p. 8, 2018.
[23] I. Ahmad, "Integrated neuro-evolution-based computing solver for dynamics of nonlinear corneal shape model numerically," *Neural Computing & Applications*, vol. 33, 2020.
[24] M. Shoaib, M. A. Z. Raja, M. T. Sabir et al., "A stochastic numerical analysis based on hybrid NAR-RBFs networks nonlinear SITR model for novel COVID-19 dynamics," *Computer Methods and Programs in Biomedicine*, vol. 202, Article ID 105973, 2021.
[25] T. N. Cheema, M. A. Z. Raja, I. Ahmad, S. Naz, H. Ilyas, and M. Shoaib, "Intelligent computing with Levenberg–Marquardt artificial neural networks for nonlinear system of COVID-19 epidemic model for future generation disease control," *The European Physical Journal Plus*, vol. 135, no. 11, pp. 932–935, 2020.
[26] M. Shoaib, M. A. Z. Raja, M. A. R. Khan, I. Farhat, and S. E. Awan, "Neuro-computing networks for entropy generation under the influence of MHD and thermal radiation," *Surfaces and Interfaces*, vol. 25, Article ID 101243, 2021.
[27] M. Shoaib, M. A. Z. Raja, W. Jamshed, K. S. Nisar, I. Khan, and I. Farhat, "Intelligent computing Levenberg Marquardt approach for entropy optimized single-phase comparative study of second grade nanofluidic system," *International Communications in Heat and Mass Transfer*, vol. 127, Article ID 105544, 2021.
[28] RA. Khan, H. Ullah, M. A. Z. Raja, M. A. R. Khan, S. Islam, and M. Shoaib, "Heat transfer between two porous parallel plates of steady nanofludis with Brownian and Thermophoretic effects: a new stochastic numerical approach," *International Communications in Heat and Mass Transfer*, vol. 126, Article ID 105436, 2021.
[29] I. Khan, H. Ullah, H. AlSalman et al., "Fractional analysis of MHD boundary layer flow over a stretching sheet in porous medium: a new stochastic method," *Journal of Function Spaces*, vol. 2021, Article ID 5844741, 1 page, 2021.
[30] I. Khan, H. Ullah, H. AlSalman et al., "Falkner–skan equation with heat transfer: a new stochastic numerical approach," *Mathematical Problems in Engineering*, vol. 2021, Article ID 3921481, 1 page, 2021.
[31] H. Bilal, H. Ullah, M. Fiza et al., "A Levenberg-Marquardt backpropagation method for unsteady squeezing flow of heat and mass transfer behaviour between parallel plates," *Advances in Mechanical Engineering Advances in Mechanical Engineering*, vol. 13, no. 10, pp. 168781402110408–168781402110415, 2021.
[32] H. Ullah, I. Khan, M. Fiza et al., "MHD boundary layer flow over a stretching sheet: a new stochastic method," *Mathematical Problems in Engineering*, vol. 2021, Article ID 9924593, 1 page, 2021.
[33] H. Ullah, I. Khan, H. AlSalman et al., "Levenberg–marquardt backpropagation for numerical treatment of micropolar flow in a porous channel with mass injection," *Complexity*, vol. 2021, Article ID 5337589, 1 page, 2021.
[34] M. Shoaib, M. Kausar, M. I. Khan et al., "Intelligent backpropagated neural networks application on Darcy-Forchheimer ferrofluid slip flow system," *International Communications in Heat and Mass Transfer*, vol. 129, Article ID 105730, 2021.
[35] M. Shoaib, M. Kausar, K. S. Nisar, M. A. Z. Raja, M. Zeb, and A. Morsy, "The design of intelligent networks for entropy

generation in Ree-Eyring dissipative fluid flow system along quartic autocatalysis chemical reactions," *International Communications in Heat and Mass Transfer*, vol. 133, Article ID 105971, 2022.

[36] M. Shoaib, G. Zubair, K. S. Nisar et al., "Ohmic heating effects and entropy generation for nanofluidic system of Ree-Eyring fluid: intelligent computing paradigm," *International Communications in Heat and Mass Transfer*, vol. 129, Article ID 105683, 2021.

[37] R. Ellahi and A Riaz, "Analytical solutions for MHD flow in a third-grade fluid with variable viscosity," *Mathematical and Computer Modelling*, vol. 52, no. 9-10, pp. 1783–1793, 2010.

[38] A. Riaz, A. Zeeshan, and M. M. Bhati, "Entropy analysis of a three dimensional wavy flowof erying powell nanofluid," *Math.Prob.Eng*, vol. 2021, Article ID 6672158, 2021.

[39] A. Riaz, A. Razaq, and A. U. Awan, "Magnetic field and permeability effects on Jeffrey fluid in eccentric tubes having flexible porous boundaries," *Journal of Magnetics*, vol. 22, no. 4, pp. 642–648, 2017.

[40] A. Zeeshan, N Ijaz, A Riaz, A. B. Mann, and A. Hobiny, "Flow of nonspherical nanoparticles in electro-magnetohydrodynamics of nanofluids through a porous medium between eccentric cylinders," *Journal of Porous Media*, vol. 23, no. 12, pp. 1201–1212, 2020.